

The Influence of Char Preparation and Biomass Type on Char Steam Gasification Kinetics

Authors:

Tilia Dahou, Françoise Defoort, Sébastien Thiéry, Maguelone Grateau, Matthieu Campargue, Simona Bennici, Mejdj Jeguirim, Capucine Dupont

Date Submitted: 2018-09-21

Keywords: thermogravimetric analysis, characteristic time analysis, kinetics, pyrolysis conditions, steam gasification, Biomass

Abstract:

A study was conducted to investigate the parameter that has influence on steam gasification kinetics between the biomass type and char preparation. Thermogravimetric analysis (TGA) was carried out on steam gasification of seven biomass samples as well as chars from three of these samples. Chars were prepared using three different sets of low heating rate (LHR) pyrolysis conditions including temperature and biomass bed geometry. It was shown by a characteristic time analysis that these pyrolysis conditions were not associated with a chemical regime in a large amount of devices. However, it has been shown experimentally that conditions used to prepare the char had a much lower influence on steam gasification kinetics than the biomass type.

Record Type: Published Article

Submitted To: LAPSE (Living Archive for Process Systems Engineering)

Citation (overall record, always the latest version):

LAPSE:2018.0647

Citation (this specific file, latest version):

LAPSE:2018.0647-1

Citation (this specific file, this version):



LAPSE:2018.0647-1v1

DOI of Published Version: <https://doi.org/10.3390/en11082126>

License: Creative Commons Attribution 4.0 International (CC BY 4.0)

Article

The Influence of Char Preparation and Biomass Type on Char Steam Gasification Kinetics

Tilia Dahou ^{1,2,3,*} , Françoise Defoort ¹, Sébastien Thiéry ¹, Maguelone Grateau ¹,
Matthieu Campargue ⁴, Simona Bennici ², Mejdı Jeguirim ²  and Capucine Dupont ⁵

¹ Université Grenoble Alpes, CEA, LITEN, DTBH, 17 avenue des Martyrs, 38054 Grenoble CEDEX 09, France; francoise.defoort@cea.fr (F.D.); sebastien.thiery@cea.fr (S.T.); maguelone.grateau@cea.fr (M.G.)

² Institut de Sciences des Matériaux de Mulhouse, UMR 7661 CNRS, 15 rue Jean-Starcky, 68057 Mulhouse CEDEX, France; simona.bennici@uha.fr (S.B.); mejdi.jeguirim@uha.fr (M.J.)

³ Agence de l'Environnement et de la Maîtrise de l'Energie (ADEME), 20 avenue du Grésillé, BP 90406, 49004 Angers CEDEX 01, France

⁴ RAGT Energie, Zone Innoprod, Chemin de la Teulière, 81012 Albi CEDEX 9, France; mcampargue@ragt.fr

⁵ IHE Delft Institute for Water Education, Westvest 7, 2611 AX Delft, The Netherlands; c.dupont@un-ihe.org

* Correspondence: tilia.dahou@cea.fr; Tel.: +33-4-38-78-54-69

Received: 23 July 2018; Accepted: 14 August 2018; Published: 15 August 2018



Abstract: A study was conducted to investigate the parameter that has influence on steam gasification kinetics between the biomass type and char preparation. Thermogravimetric analysis (TGA) was carried out on steam gasification of seven biomass samples as well as chars from three of these samples. Chars were prepared using three different sets of low heating rate (LHR) pyrolysis conditions including temperature and biomass bed geometry. It was shown by a characteristic time analysis that these pyrolysis conditions were not associated with a chemical regime in a large amount of devices. However, it has been shown experimentally that conditions used to prepare the char had a much lower influence on steam gasification kinetics than the biomass type.

Keywords: biomass; steam gasification; kinetics; pyrolysis conditions; thermogravimetric analysis; characteristic time analysis

1. Introduction

Today, there is a consensus about the increasing need of biomass use for energy applications. Given the limited availability of wood, it seems essential to identify and to convert other biomass resources such as agricultural co-products. Among the various techniques for biomass conversion to energy, the gasification process is a promising one [1] such as in the case of hydrogen production [2–4] or liquid fuel synthesis [5–7]. This process includes two main steps that can overlap: biomass pyrolysis leading to char formation and gasification of the char producing syngas, i.e., a gas mixture of mainly CO and H₂. It has been shown that, with steam as a gasifying agent, the char gasification reaction has the slowest reaction under typical operating conditions [8]. Therefore, the design of industrial gasifiers requires the understanding and control of the steam gasification kinetics.

Since char is the starting material for gasification, it is important to identify the main parameter affecting char gasification kinetics.

In literature, two charring parameters are identified as having a potential influence on the steam gasification kinetics including pyrolysis operating conditions and biomass type [9]. The influence of pyrolysis conditions is largely related to the heating rate. Differences are especially noted between slow pyrolysis—low heating rate (LHR), <50 °C·min⁻¹—and fast pyrolysis—high heating rate (HHR), 500 °C·min⁻¹ [10]. The steam gasification rate increases when the heating rate increases, which is

linked to char morphology differences. During LHR pyrolysis, the char keeps its natural porosity while, in HHR pyrolysis, larger cavities are formed [9]. This larger surface area in the case of HHR pyrolysis along with the higher content in oxygen and hydrogen results in more available active sites [11]. The influence of the biomass type is basically related to the inorganic elements content of the biomass [12], which can attain high values for some resources such as agricultural residues [13]. In particular, alkali and alkaline earth metals (AAEMs) have a catalytic effect on gasification [14–17]. In contrast, elements such as silicon or phosphorus have an inhibiting effect [18,19].

To explain the origin of the influence of these two parameters, the first step is to determine the regime of the transformation, i.e., the phenomenon—chemical reaction or transfer—limiting its kinetics. Char preparation in conditions outside the chemical regime could result in variations in the properties of the chars. Differences between the chars obtained could lead to differences between their gasification behaviors. The regime of the transformation can be assessed through an analysis of the characteristic times of the phenomena involved. In literature, such an analysis has already been conducted by several authors. For instance, this can include pyrolysis [20–24], pyrogasification [8], and torrefaction [25] at the particle scale. However, most of these studies were performed for fast pyrolysis (HHR) and not slow pyrolysis (LHR). Moreover, time scale analysis is usually applied to a particle (for micrometric to centimetric scale particles), but more rarely to a bed of fine particles. One example can be found for torrefaction for which Gonzalez Martinez et al. [25] performed such an analysis at particle as well as at bed scale.

The present work combines the analysis of these characteristic times both at a particle scale and at a bed scale and an experimental study through thermogravimetric analysis (TGA). It focuses on slow pyrolysis (LHR) conditions (10 to 24 °C·min⁻¹) and parameters as the amount of biomass treated, i.e., geometry (height and surface) of the crucible and the working temperature (450 °C or 800 °C in one or two steps). Gasification was carried out on seven biomass samples as well as on chars prepared from three of these samples in four different sets of conditions. It aims to assess the relative influence of the two parameters previously discussed including char preparation conditions and biomass type on steam gasification kinetics.

2. Materials and Methods

2.1. Biomass Samples

Seven biomass samples covering a variety of compositions were selected for this study. The selection mainly includes agricultural residues. Samples were ground below 200 µm in a rotor mill. The ash content and inorganic element composition of the samples was measured, according to solid fuel standards NF EN 14775 [26] and NF EN ISO 16967 [27], respectively. Values obtained for each biomass sample can be found in Table 1. From these values, the three main inorganic elements in mass were identified.

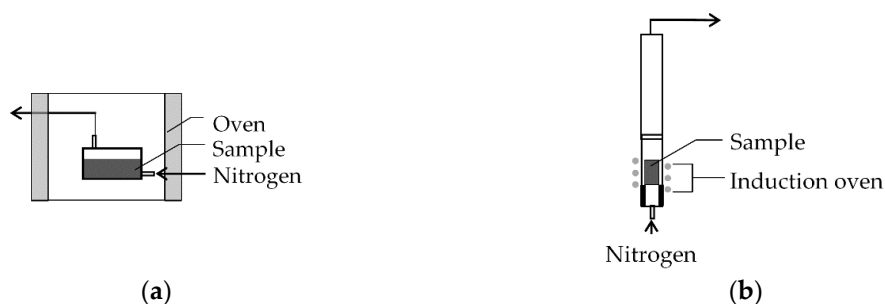
The main inorganic elements contained in all biomasses are Ca and K. The third main element is Si, Mg, or P. Rice husk and wheat straw can be classified as silica-rich. Sunflower seed shells and alfalfa have a high potassium content. The others are rich in calcium.

Table 1. Ash and inorganic element content of the biomass samples (on dry basis).

Biomass Sample	Rice Husk	Wheat Straw [28]	Apple Orchard Residue [28]	Apricot Orchard Residue [28]	Vineyard Residue [28]	Sunflower Seed Shells	Alfalfa
Ash at 550 °C (wt %)	14.1	6.8	3.8	3.7	2.6	3.3	7.8
Si (mg·kg ⁻¹)	60,750	20,757	820	990	1012	258	510
K (mg·kg ⁻¹)	5363	13,063	3771	7254	5045	12,926	25,695
Ca (mg·kg ⁻¹)	1718	5627	9472	10,927	7808	6392	9694
Mg (mg·kg ⁻¹)	538	693	872	1374	1604	2812	1123
P (mg·kg ⁻¹)	630	1373	1325	1161	1011	1323	2997
Na (mg·kg ⁻¹)	270	164	25	41	37	20	289
Al (mg·kg ⁻¹)	166	429	71	104	151	257	83
Fe (mg·kg ⁻¹)	163	299	58	88	113	233	109
Mn (mg·kg ⁻¹)	183	50	11	20	42	12	<11
Main Inorganic Elements	Si	Si	Ca	Ca	Ca	K	K
	K	K	K	K	K	Ca	Ca
	Ca	Ca	P	Mg	Mg	Mg	P

2.2. Char Preparation

LHR pyrolysis in 1 L·min⁻¹ N₂ was carried out in three different sets of conditions in order to prepare large amounts of char from the different biomass feedstocks. Two devices were used to carry out the pyrolysis. They are illustrated in Figure 1.

**Figure 1.** (a) Device M used for pyrolysis; (b) Device P used for pyrolysis.

Device M consists of a sample holder swept by nitrogen and placed in an oven. It can be used for large quantities of sample (30 g to 50 g depending on biomass) but only operates at moderate temperatures (450 °C). Device P consists of a mesh basket sample holder placed in a tube swept by nitrogen and heated by induction. It can reach higher temperatures (800 °C), but a lower amount of sample (approximately 5 g) can be converted at once.

Each set of conditions for char preparation from the biomass samples is described in Table 2. The first set of conditions (char M) is at a low temperature (450 °C) while the two other sets of conditions (char M-P and char P-P) have two temperature steps (450 °C and 800 °C) in the same or different devices.

In addition, char was produced from in-situ pyrolysis of the biomass before gasification in the thermo-balance (see following section), which pyrolysis conditions (char TGA) are listed in Table 2.

Table 2. Pyrolysis conditions for char preparation from the biomass samples.

	Char TGA	Char M	Char M-P	Char P-P
Device for treatment at 450 °C	TGA	Device M	Device M	Device P
Sample holder dimension at 450 °C height × diameter (mm × mm)	2.5 × 7	40 × 70	40 × 70	48 × 32
Heating rate to 450 °C (°C·min ⁻¹)	24	10	10	24
Holding time at 450 °C (min)	60	60	60	60
Cooling between treatment at 450 °C and 800 °C	No	–	Yes	No
Device for treatment at 800 °C	TGA	–	Device P	Device P
Heating rate to 800 °C (°C·min ⁻¹)	24	–	24	24
Holding time at 800 °C (min)	30	–	30	30

TGA: thermogravimetric analysis.

2.3. Steam Gasification Reactivity

Steam gasification reactivities of the four types of char (Table 2) were obtained through thermogravimetric analysis (TGA). Experiments were carried out at an atmospheric pressure using a Setsys thermobalance (SETARAM, Caluire, France) coupled with a Wetsys steam generator. For chars M, M-P, and P-P, which is a mass of 3 mg to 4 mg—i.e., the mass experimentally determined to be independent from heat and mass transfer influence—was placed in a cylindrical crucible of 2.5 mm height and 7 mm diameter. Samples were heated at 24 °C·min⁻¹ until 800 °C under 0.05 L·min⁻¹ N₂ except for char TGA, which starting material was biomass and for which an intermediate step at 450 °C was performed, which is shown in Table 2. In this last case, a mass of 14 mg of biomass was placed in the crucible. Samples were swept by N₂ for 45 min after the final temperature was reached to ensure pyrolysis completion and mass stability. Gas was then switched to a mixture of 20 vol % H₂O in N₂.

Steam gasification reactivities of the biomass samples were also measured. It corresponds to the preparation of char TGA described in the previous section, which is directly followed by steam gasification. The experimental procedure was similar to the one used for chars.

A solid conversion was then defined from mass loss measured as a function of time during TGA by using the following expression.

$$X = \frac{m_i - m(t)}{m_i - m_f}, \quad (1)$$

where m_i , $m(t)$, and m_f are the masses of char before gasification (at the time of steam injection) at the time t and at the end of gasification (remaining ash), respectively.

The gasification rate could then be defined as the variation of conversion versus the equation below.

$$r = X \frac{dX}{dt}. \quad (2)$$

An average reactivity between two values of conversion X_1 and X_2 was also defined below.

$$r_{X_1-X_2} = \frac{\int_{t_{X_1}}^{t_{X_2}} \frac{r(t)dt}{1-X(t)}}{t_{X_2} - t_{X_1}}. \quad (3)$$

2.4. Characteristic Time Calculation

The characteristic time of a phenomenon is the theoretical time needed for a process to occur when it is only controlled by this phenomenon [29]. It depends on the operating conditions. Phenomena to consider can be chemical reactions, heat transfers, mass transport, or other phenomena. From comparing characteristic times, the limiting phenomenon can be identified and the regime of the process can be defined.

In this study, characteristic times were calculated for char preparation through pyrolysis and for steam gasification of the char to represent the chosen experimental procedure as closely as possible in which the two reactions occur one after the other. Analysis of the characteristic times of the pyrolysis step is important since, if other phenomena than the chemical reaction occur, it could result in the production of different chars in the different conditions. Since char is the starting material to gasification, it could mean that these chars would behave differently during gasification. Analysis of the characteristic times of the gasification step is meant to validate the results from steam gasification TGA since reactivities are meaningful only in a chemical regime, i.e., when the chemical reaction is the leading phenomenon.

Phenomena involved in each process are illustrated in Figure 2.

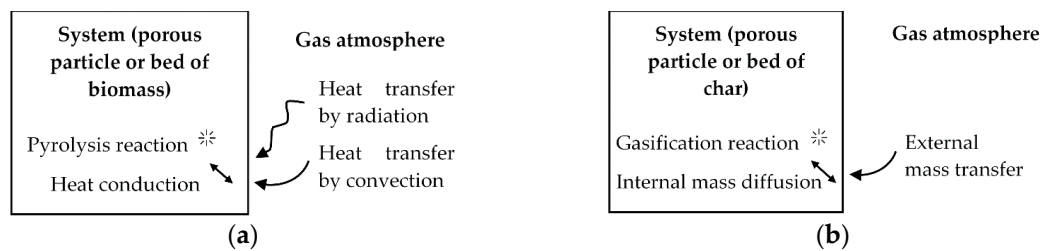


Figure 2. (a) Phenomena involved in pyrolysis; (b) Phenomena involved in gasification.

In the case of pyrolysis, the process is not led under isothermal conditions. Therefore, the characteristic times of the phenomena were compared to the heating time.

Characteristic times of each phenomenon as well as heating time are defined in Tables 3 and 4 for pyrolysis and gasification, respectively.

Table 3. Characteristic time definition for the pyrolysis of biomass.

Phenomenon	Definition of Characteristic Time
Pyrolysis chemical reaction	$t_{pyro} = \frac{1}{k_{pyro}}$
External heat transfer by convection	$t_{conv} = \frac{\rho_{solid} c_p \text{ solid } L_c}{h_t}$
External heat transfer by radiation	$t_{rad} = \frac{\rho_{solid} c_p \text{ solid } L_c}{\omega_{solid} \sigma (T_{gas} + T_{solid}) (T_{gas}^2 + T_{solid}^2)}$
Internal heat transfer by conduction	$t_{cond} = \frac{\rho_{solid} c_p \text{ solid } L_c^2}{\lambda_{solid}}$
Heating	$t_{heating} = \frac{T_{gas} - T_{solid}}{r_{heating}}$

Table 4. Characteristic time definition for the gasification of biomass.

Phenomenon	Definition of Characteristic Time
Gasification chemical reaction	$t_{gasif} = \frac{1}{k_{gasif}}$
External mass transfer	$t_{mass \ ext} = \frac{\rho_{solid} R T_{gas} L_c}{h_m P_{H_2O} M_{H_2O}}$
Internal mass diffusion	$t_{diff \ int} = \frac{L_c^2}{D_{eff}}$

Pyrolysis and gasification chemical reactions of kinetic parameters were taken from literature. Pyrolysis kinetic parameters were taken from Di Blasi's review [30]: results were calculated both for the fastest [31] and the slowest [32] laws. For gasification, a law taking into account biomass composition was chosen [18]. Among a fast-reacting biomass, alfalfa, and a slow reacting one, barley straw were chosen for comparison. All kinetic constants and their parameters values are gathered in Table 5.

Table 5. Kinetic constants for pyrolysis and gasification reactions.

Reaction	Kinetic Constant Expression	Biomass	k_0 (s ⁻¹)	E_a (kJ·mol ⁻¹)	$\frac{m_K}{m_{Si}}$	a	b
Pyrolysis	$k_{pyro} \exp\left(-\frac{E_a}{RT_{gas}}\right)$	Rice husk	5.8×10^{14}	200	-	-	-
		Sunflower shells	1.0×10^3	78.15	-	-	-
Gasification	$k_{gasif} \exp\left(-\frac{E_a}{RT_{gas}}\right) P_{H_2O}^{0.6} \left(a \frac{m_K}{m_{Si}} + b\right)$	Barley straw	8.8×10^4	167	0.1	0.18	0.59
		Alfalfa	8.8×10^4	167	50	0.18	0.59

Characteristic lengths used in characteristic time calculations are defined in Table 6.

Table 6. Characteristic lengths used for characteristic time calculations with d_p the particle diameter, D_c the bed diameter, and H_c the bed height.

System Considered	Characteristic Length L_c Definition	Device	Characteristic Length L_c Value (m)
Particle scale	$\frac{d_p}{6}$	All devices	3.3×10^{-5}
		TGA	6.3×10^{-4}
Bed scale	$\frac{D_c H_c}{2D_c + 4H_c}$	Device M	1.6×10^{-3}
		Device P	5.3×10^{-3}

Properties of the solids—biomass and char—were estimated from literature data or from our own measurements. They are gathered in Table 7.

Table 7. Physical properties of biomass and char particles and beds.

Property	Biomass Particle	Biomass Bed	Char Particle	Char Bed
Porosity ϵ_{solid} (-)	-	0.5 (estimated)	0.7 [33]	0.5 (estimated)
Tortuosity τ_{solid} (-)	-	-	3 [34]	1.57 [35]
Density ρ_{solid} (kg·m ⁻³)	860	430 (measured)	400 (estimated)	200
Specific heat $c_{p, solid}$ (J·kg ⁻¹ ·K ⁻¹)	1266 [36]	1266	-	-
Thermal conductivity λ_{solid} (W·m ⁻¹ ·K ⁻¹)	0.18 [37]	0.09	-	-
Emissivity ω_{solid} (-)	0.9 [37]	0.9	-	-

Lastly, transfer coefficients were obtained from correlations from literature. They use gas properties from literature [37] and are defined in Table 8.

Table 8. Definition of transfer coefficients.

Transfer Coefficient	Coefficient Definition	Correlation
Heat transfer coefficient h_t (W·m ⁻² ·K ⁻¹)	$\frac{\lambda_{gas} Nu}{L_c}$	$Nu = 2 + \left(0.4Re^{\frac{1}{2}} + 0.06Re^{\frac{2}{3}}\right) Pr^{0.4}$ [38]
Effective diffusion coefficient D_{eff} (m ² ·s ⁻¹)	$\frac{\epsilon_{solid}}{\tau_{solid}} D_{H_2O-N_2}$	$D_{H_2O-N_2} = \frac{0.001 T_{gas}^{1.75} \left(\frac{1}{M_{H_2O}} + \frac{1}{M_{N_2}}\right)^{\frac{1}{2}}}{P_{gas} \left((\Sigma v)_{H_2O}^{\frac{1}{3}} + (\Sigma v)_{N_2}^{\frac{1}{3}}\right)^2}$ [39]
Mass transfer coefficient h_m (m·s ⁻¹)	$\frac{D_{H_2O-N_2} Sh}{L_c}$	$Sh = 2 + \left(0.4Re^{\frac{1}{2}} + 0.06Re^{\frac{2}{3}}\right) Sc^{0.4}$ [38]

Gas properties have a satisfactory accuracy while biomass and char properties as well as heat and mass transfer coefficients and kinetic parameters are estimated or calculated from empirical equations. Therefore, this low accuracy on the values used for calculations must be taken into account when analyzing the results obtained for characteristic times.

3. Results and Discussion

The experimental method used to demonstrate the influence of char preparation and biomass type involves various experimental devices at different scales. Therefore, it is necessary to look at the time scales of the phenomena involved in the process to determine its regime, i.e., chemical regime or regime led by heat or mass transfer. The analysis was conducted separately on pyrolysis and on gasification since these two steps were experimentally separated.

3.1. Characteristic Time Analysis

3.1.1. Analysis of Characteristic Times of the Pyrolysis Step

Characteristic times of the pyrolysis step are represented in Figure 3 for particle scale and for bed scale in the conditions of TGA, device M, and device P for a particle size below 200 μm . Results are shown as a function of temperature between 200 $^{\circ}\text{C}$ and 450 $^{\circ}\text{C}$, i.e., in the range of temperature corresponding to biomass degradation, according to the literature [40].

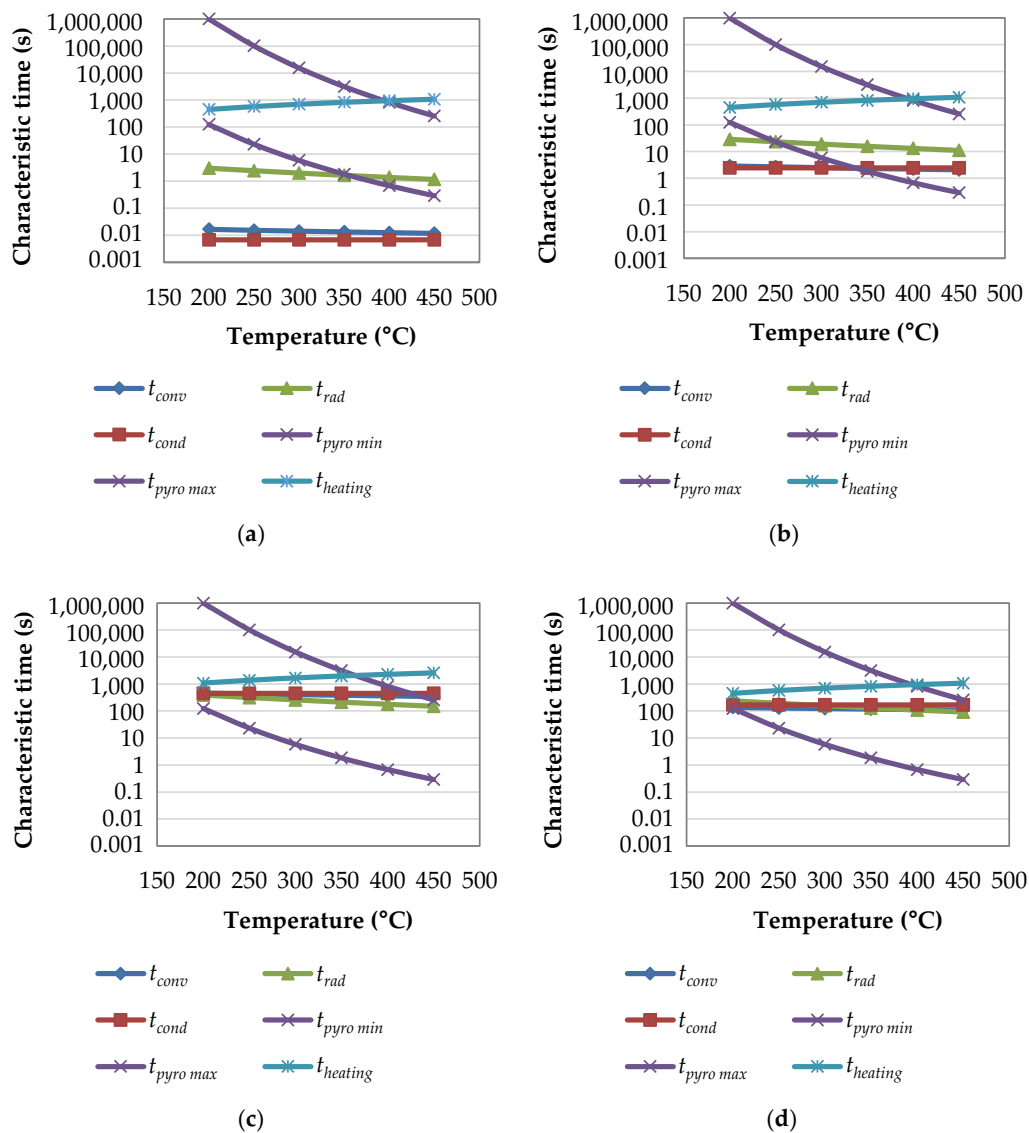


Figure 3. Characteristic times of the pyrolysis step as a function of temperature for: (a) particle scale in TGA conditions; (b) bed scale in TGA conditions; (c) bed scale in device M conditions; and (d) bed scale in device P condition. TGA: thermogravimetric analysis.

Calculations at particle scale were carried out for each of the three device conditions but results showed very negligible differences that were not noticeable through graphical representation. Therefore, only results obtained from TGA conditions are presented in this paper.

In all four cases, heating time and pyrolysis reaction times are the same except for heating time in device M conditions, but its variation is negligible. Only the three heat transfer characteristic times vary since they depend on the geometry of the system. Clearly, these characteristic times increase when the scale of the system—particle and beds of different sizes—increases.

When comparing heat transfers to the pyrolysis chemical reaction, it can be seen that their characteristic times are of the same order magnitude at least in part of the temperature range. This indicates that these phenomena occur simultaneously and none can be neglected.

Moreover, since pyrolysis was experimentally carried out in a dynamic mode, these times need to be compared with the heating time. For the phenomena to have enough time to occur, heating time should be higher than the phenomena characteristic times. In this study, heating times chosen for preparing the chars are of the same order of magnitude as the characteristic times of the phenomena involved.

In conclusion, characteristic time analysis shows that the pyrolysis step does not occur in a chemical regime. All phenomena occur simultaneously—none of them is negligible—and heating is too fast for the phenomena to occur.

Not being in a chemical regime during pyrolysis could result in chars that have different properties. Having different starting materials for gasification could, therefore, induce different kinetic behaviors. This is why it is important to check experimentally that chars produced under various conditions give the same gasification kinetics.

3.1.2. Analysis of Characteristic Times of the Gasification Step

Characteristic times of the gasification step are represented in Figure 4 for particle scale and bed scale under TGA conditions. Results are shown as a function of temperature between 500 °C and 1000 °C with the experimental study carried out at 800 °C in our study.

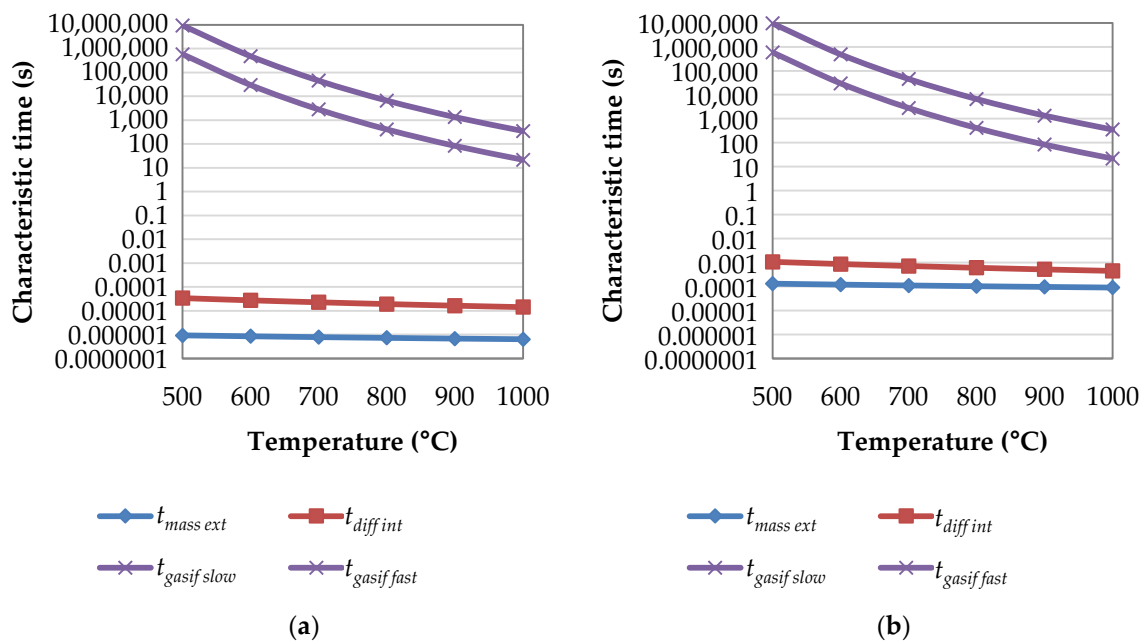


Figure 4. Characteristic times of the gasification step as a function of temperature for TGA conditions at: (a) particle scale and (b) bed scale.

At both scales, gasification chemical reactions with characteristic times remain the same. Mass transfer times slightly increase when the scale increases. However, at both scales and for both gasification kinetic laws, the gasification chemical reaction times are significantly higher—five to eight orders of magnitude—than mass transfer times. Therefore, according to time scales analysis, the gasification chemical reaction is the limiting phenomenon and mass transfers are negligible in comparison. The process occurs in the chemical regime.

This result is important since it means that kinetics obtained through TGA in these conditions should be intrinsic. According to this analysis, they exclusively represent the gasification chemical reaction without any bias from mass transfers.

However, Di Blasi's review [9] states that, even in TGA, typical operating condition mass transfers can have a non-negligible effect on char gasification. To verify this result experimentally for the conditions of the work presented in this study, gasification was carried out on different masses of the same char sample ranging from the full crucible (14 mg) to 3 mg. Only gasification of 4 mg or below showed the same kinetics. Higher masses of samples reacted more slowly, which indicated mass transfer limitations. These observations were close to previous results obtained on the same apparatus under similar conditions [12]. It shows the limits of characteristic time analysis, which relies on parameters known with limited accuracy.

3.2. Influence of Biomass Type

The influence of the biomass type on gasification kinetics was investigated through TGA of the biomass samples, i.e., preparation of char TGA and gasification of this char. Results from the mass loss as a function of time in these experiments are presented in Figure 5. Replicates are not shown in this paper but were carried out to ensure repeatability of the process, which was validated—variability can be seen in Figure 6 through error bars.

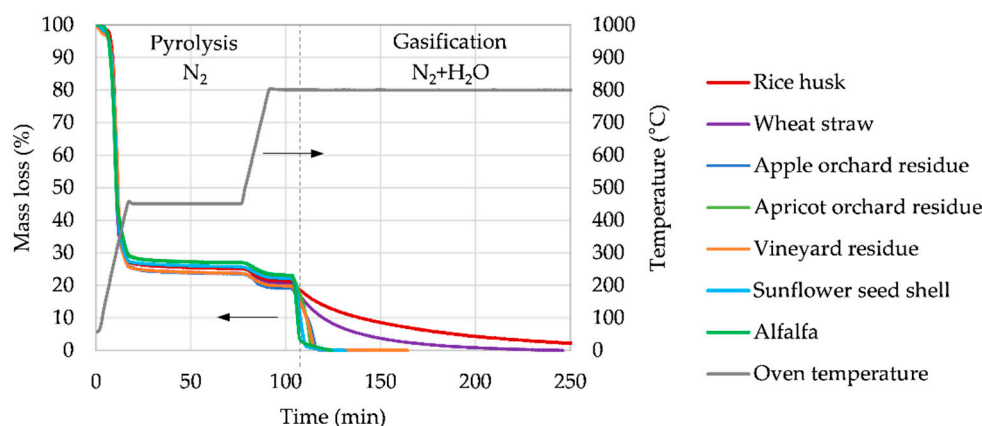


Figure 5. TGA of biomass samples presented as a mass loss and as a function of time. Pyrolysis: $0.05 \text{ L}\cdot\text{min}^{-1} \text{ N}_2$, $24 \text{ }^\circ\text{C}/\text{minutes}$, 1 h hold at $450 \text{ }^\circ\text{C}$, 15-min hold at $800 \text{ }^\circ\text{C}$. Gasification: $0.05 \text{ L}\cdot\text{min}^{-1}$ mixture 80 vol % $\text{N}_2/20 \text{ vol } \% \text{ H}_2\text{O}$, $800 \text{ }^\circ\text{C}$.

It can be noted that mass loss profiles obtained during the pyrolysis of biomass samples are very similar.

The highest mass loss is observed for temperatures below $450 \text{ }^\circ\text{C}$ with approximately 75% of the mass volatilized. Subsequently, around 5% of the mass is lost between $450 \text{ }^\circ\text{C}$ and $800 \text{ }^\circ\text{C}$. These yields align with results from literature [41]. They can be compared with char yields obtained after pyrolysis in other devices used for char preparation, which are gathered in Figure 6.

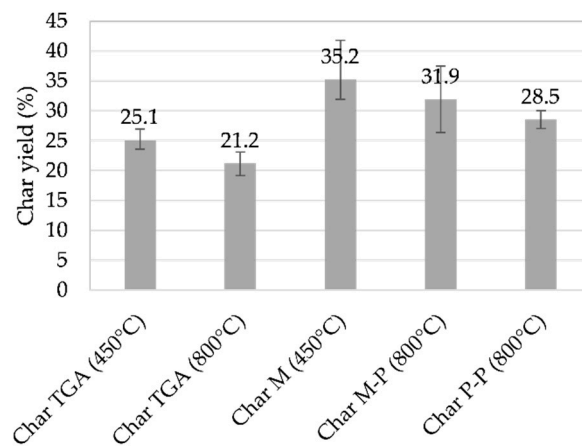


Figure 6. Char yield obtained in each char preparation condition (see Table 2).

There is a visible difference between values obtained at the thermo-balance scale and values obtained on devices M and P. This observation might be due to heat transfer limitations that are higher in the devices M and P, which are seen with characteristic times and can result in a lower solid conversion, i.e., a higher char yield. However, large scale values are close to what is expected for slow pyrolysis at pilot or industrial scale—35% char, 30% condensable products, and 35% non-condensable products [40,42].

The focus is made on the gasification step in Figure 7 and presented as a solid conversion and as a function of time.

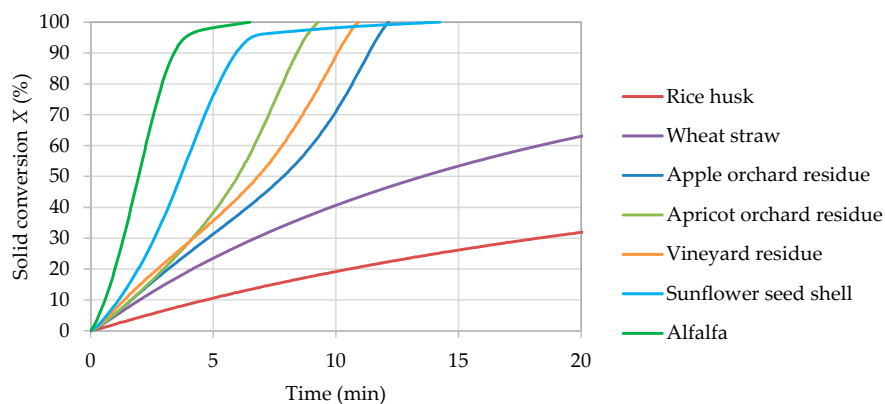


Figure 7. Solid conversion of biomass samples as a function of time during the gasification step (char TGA, $0.05 \text{ L}\cdot\text{min}^{-1}$ mixture 80 vol % N_2 /20 vol % H_2O , 800°C). Including data from Dupont et al. [28].

Three families of behavior can be identified, which is identified in literature [18]:

- Family 1 and its conversion rate is the highest and is constant and then increases such as in apple orchard residue, apricot orchard residue, and vineyard residue.
- Family 2 and its conversion rate is the slowest and is continuously decreasing such as in a rice husk and wheat straw.
- Family 3 and its conversion rate is intermediate and is constant and then decreases such as in sunflower seed shells and in alfalfa.

In addition, average reactivities of these biomass samples can be compared. Values of average reactivities between 1% and 80% conversion rates are gathered in Figure 8.

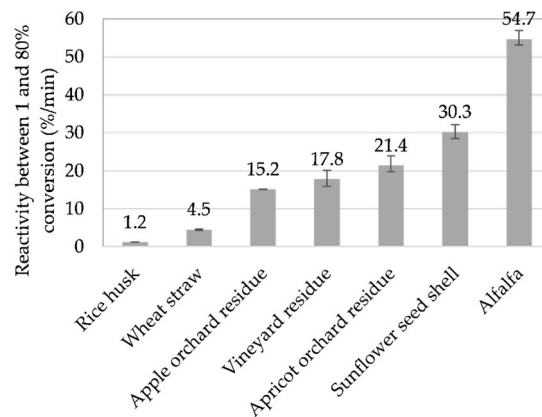


Figure 8. Gasification average reactivity between 1% and 80% conversion of biomass samples (char TGA, $0.05 \text{ L} \cdot \text{min}^{-1}$ mixture 80 vol % N_2 /20 vol % H_2O , $800 \text{ }^\circ\text{C}$).

Substantial variation between biomasses is noted due to a factor of almost 50 between average reactivities of rice husk—slowest sample to be gasified at $1.2\% \cdot \text{min}^{-1}$ —and alfalfa—fastest sample to be gasified at $54.7\% \cdot \text{min}^{-1}$.

These results could be related to inorganic composition of biomass samples. Silica-rich samples tended to have lower reaction rates than silica-poor samples. Among the latter, the reaction rate tends to increase with increasing content of potassium, which is in accordance with literature [18,43]. Other physicochemical characterizations such as a surface area measurement or H and O quantification have not been performed in the present study and may bring a better understanding of the results.

3.3. Influence of Char Preparation

To investigate the influence of char preparation, steam gasification kinetics of chars prepared in different conditions were compared. To carry out this comparison, samples with extreme behaviors were selected from the study of biomass samples. Sunflower seed shells and alfalfa were chosen for their high reactivity, high potassium content, and low silicon content. The rice husk was chosen for its low reactivity, low potassium content, and high silicon content.

TGA of the gasification step was conducted on this chars selection. Results expressed in the form of solid conversion as a function of time are presented in Figure 9. Reactivities between 1% and 80% were derived from these results and are given in Figure 10.

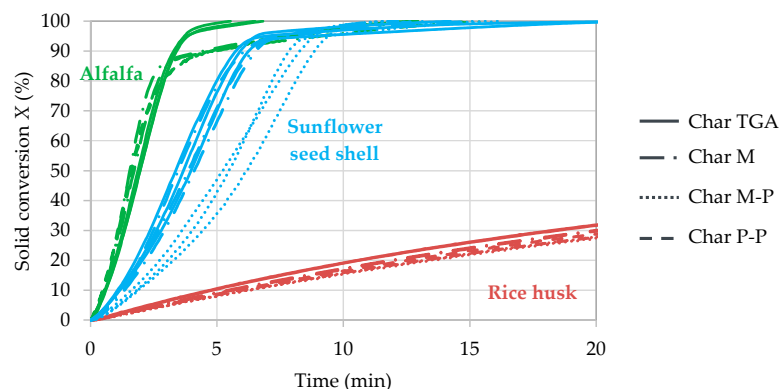


Figure 9. Solid conversion of chars as a function of time during gasification ($0.05 \text{ L} \cdot \text{min}^{-1}$ mixture 80 vol % N_2 /20 vol % H_2O , $800 \text{ }^\circ\text{C}$).

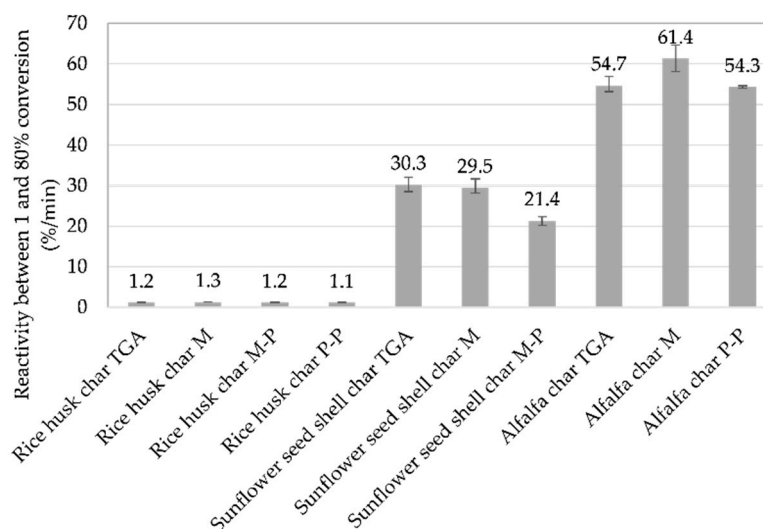


Figure 10. Gasification average reactivity between 1% and 80% conversion of biomass and char samples (see Table 2).

For each biomass, chars prepared in different conditions—in particular LHR pyrolysis conditions and not in a chemical regime—have the same reactivity during gasification. One exception for char M-P comes from the sunflower seed shells. No explanation was found regarding this result but it may be found by characterizing the chars. However, variations are negligible compared to differences that are observed between fast-reacting and slow-reacting biomass types. There is a factor of 1.2 in average between reactivities of the various char samples from each biomass, which is very low when compared to the factor of almost 50 calculated between reactivities of rice husk and alfalfa.

4. Conclusions

Thermogravimetric analysis (TGA) of biomass samples and of chars prepared from these biomasses in different LHR pyrolysis conditions outside the chemical regime showed that the biomass type has a significantly higher influence on steam gasification kinetics than char preparation conditions. In the range of the seven studied biomass samples, a factor of almost 50 was measured between average reactivities of the two samples with extreme behavior (rice husk with $1.2\% \cdot \text{min}^{-1}$ and alfalfa with $54.7\% \cdot \text{min}^{-1}$). In comparison, chars prepared in conditions outside the chemical regime from various amounts of biomass depending on the crucible geometry (height and surface) and several working temperatures ($450\text{ }^{\circ}\text{C}$ or $800\text{ }^{\circ}\text{C}$ in one or two steps) showed a much lower difference with an average factor of 1.2 for a given biomass type.

The influence of biomass type could be assumed to be related to inorganic content of the biomass as opposed to its molecular constituents—lignin, hemicellulose, cellulose. This assumption is supported by literature data. However, further investigations are in progress and consist of physicochemical characterization of chars from different biomass samples. It will confirm if inorganic composition is the main influential parameter or if it should rather be explained by structural or textural properties of the char.

Author Contributions: Conceptualization, F.D., M.C., S.B., M.J. and C.D. Investigation, T.D., S.T. and M.G. Formal Analysis, T.D. Resources, M.C. Writing-Original Draft Preparation, T.D. Writing-Review & Editing, F.D., M.J. and C.D. Supervision, F.D., M.J. and C.D.

Funding: This research was funded by the Agence de l'Environnement et de la Maîtrise de l'Energie.

Conflicts of Interest: The authors declare no conflict of interest.

Nomenclature

$c_{p\ solid}$	$(\text{J}\cdot\text{kg}^{-1}\cdot\text{K}^{-1})$	Specific heat of the solid phase (bed or particle)
d_p	(m)	Particle diameter
D_c	(m)	Diameter of the cylindrical bed
D_{eff}	$(\text{m}^2\cdot\text{s}^{-1})$	Effective diffusion coefficient
$D_{H_2O-N_2}$	$(\text{m}^2\cdot\text{s}^{-1})$	Diffusion coefficient of the mixture $\text{N}_2\text{-H}_2\text{O}$
h_m	$(\text{m}\cdot\text{s}^{-1})$	External mass transfer coefficient
h_t	$(\text{W}\cdot\text{m}^{-2}\cdot\text{K}^{-1})$	Heat transfer coefficient
H_c	(m)	Height of the cylindrical bed
k_{gasif}	(s^{-1})	Kinetic constant of the gasification reaction
k_{pyro}	(s^{-1})	Kinetic constant of the pyrolysis reaction
M_{H_2O}	$(\text{kg}\cdot\text{mol}^{-1})$	Molecular weight of water
M_{N_2}	$(\text{kg}\cdot\text{mol}^{-1})$	Molecular weight of nitrogen
Nu	(–)	Nusselt number
P_{H_2O}	(Pa)	Partial pressure of steam
P_{gas}	(Pa)	Pressure of the gas
Pr	(–)	Prandtl number
r	(s^{-1})	Gasification rate
$r_{heating}$	$(\text{K}\cdot\text{s}^{-1})$	Heating rate
R	$(\text{J}\cdot\text{mol}^{-1}\cdot\text{K}^{-1})$	Universal gas constant
Re	(–)	Reynolds number
Sc	(–)	Schmidt number
Sh	(–)	Sherwood number
t_{cond}	(s)	Internal heat conduction time
t_{conv}	(s)	External heat convection time
$t_{diff\ int}$	(s)	Characteristic time of internal mass diffusion
t_{gasif}	(s)	Characteristic time of the gasification chemical reaction
$t_{heating}$	(s)	Heating time
$t_{mass\ ext}$	(s)	Characteristic time of external mass transfer
t_{pyro}	(s)	Characteristic time of the pyrolysis chemical reaction
t_{rad}	(s)	External radiation time
T_{gas}	(K)	Gas temperature
T_{solid}	(K)	Solid (bed or particle) temperature
X	(–)	Solid conversion
ε_{solid}	(–)	Porosity of the solid phase (bed or particle)
λ_{gas}	$(\text{W}\cdot\text{m}^{-1}\cdot\text{K}^{-1})$	Thermal conductivity of the gas phase
λ_{solid}	$(\text{W}\cdot\text{m}^{-1}\cdot\text{K}^{-1})$	Thermal conductivity of the solid phase (bed or particle)
ρ_{solid}	$(\text{kg}\cdot\text{m}^{-3})$	Density of the solid phase (bed or particle)
σ	$(\text{W}\cdot\text{m}^{-2}\cdot\text{K}^{-4})$	Boltzmann constant
$(\Sigma v)_{H_2O}$	$(\text{m}^3\cdot\text{mol}^{-1})$	Diffusion volume of H_2O
$(\Sigma v)_{N_2}$	$(\text{m}^3\cdot\text{mol}^{-1})$	Diffusion volume of N_2
τ_{solid}	(–)	Tortuosity of the solid phase (bed or particle)
ω_{solid}	(–)	Emissivity of the biomass

References

1. Kumar, A.; Jones, D.D.; Hanna, M.A. Thermochemical Biomass Gasification: A Review of the Current Status of the Technology. *Energies* **2009**, *2*, 556–581. [[CrossRef](#)]
2. Bartocci, P.; Zampilli, M.; Bidini, G.; Fantozzi, F. Hydrogen-rich gas production through steam gasification of charcoal pellet. *Appl. Therm. Eng.* **2018**, *132*, 817–823. [[CrossRef](#)]
3. Luo, S.; Xiao, B.; Guo, X.; Hu, Z.; Liu, S.; He, M. Hydrogen-rich gas from catalytic steam gasification of biomass in a fixed bed reactor: Influence of particle size on gasification performance. *Int. J. Hydrog. Energy* **2009**, *34*, 1260–1264. [[CrossRef](#)]

4. Yan, F.; Luo, S.; Hu, Z.; Xiao, B.; Cheng, G. Hydrogen-rich gas production by steam gasification of char from biomass fast pyrolysis in a fixed-bed reactor: Influence of temperature and steam on hydrogen yield and syngas composition. *Bioresour. Technol.* **2010**, *101*, 5633–5637. [[CrossRef](#)] [[PubMed](#)]
5. Rafati, M.; Wang, L.; Dayton, D.C.; Schimmel, K.; Kabadi, V.; Shahbazi, A. Techno-economic analysis of production of Fischer-Tropsch liquids via biomass gasification: The effects of Fischer-Tropsch catalysts and natural gas co-feeding. *Energy Convers. Manag.* **2017**, *133*, 153–166. [[CrossRef](#)]
6. Snehes, A.S.; Mukunda, H.S.; Mahapatra, S.; Dasappa, S. Fischer-Tropsch route for the conversion of biomass to liquid fuels—Technical and economic analysis. *Energy* **2017**, *130*, 182–191. [[CrossRef](#)]
7. Chiodini, A.; Bua, L.; Carnelli, L.; Zwart, R.; Vreugdenhil, B.; Vociante, M. Enhancements in Biomass-to-Liquid processes: Gasification aiming at high hydrogen/carbon monoxide ratios for direct Fischer-Tropsch synthesis applications. *Biomass Bioenergy* **2017**, *106*, 104–114. [[CrossRef](#)]
8. Dupont, C.; Boissonnet, G.; Seiler, J.-M.; Gauthier, P.; Schweich, D. Study about the kinetic processes of biomass steam gasification. *Fuel* **2007**, *86*, 32–40. [[CrossRef](#)]
9. Di Blasi, C. Combustion and gasification rates of lignocellulosic chars. *Prog. Energy Combust. Sci.* **2009**, *35*, 121–140. [[CrossRef](#)]
10. Ballerini, D.; Alazard-Toux, N. *Les Biocarburants*; Editions Technip: Paris, France, 2006; ISBN 978-2-7108-0969-2.
11. Guerrero, M.; Ruiz, M.P.; Millera, Á.; Alzueta, M.U.; Bilbao, R. Oxidation Kinetics of Eucalyptus Chars Produced at Low and High Heating Rates. *Energy Fuels* **2008**, *22*, 2084–2090. [[CrossRef](#)]
12. Dupont, C.; Nocquet, T.; Da Costa, J.A.; Verne-Tournon, C. Kinetic modelling of steam gasification of various woody biomass chars: Influence of inorganic elements. *Bioresour. Technol.* **2011**, *102*, 9743–9748. [[CrossRef](#)] [[PubMed](#)]
13. Vassilev, S.V.; Baxter, D.; Andersen, L.K.; Vassileva, C.G. An overview of the chemical composition of biomass. *Fuel* **2010**, *89*, 913–933. [[CrossRef](#)]
14. Feng, D.; Zhao, Y.; Zhang, Y.; Xu, H.; Zhang, L.; Sun, S. Catalytic mechanism of ion-exchanging alkali and alkaline earth metallic species on biochar reactivity during CO₂/H₂O gasification. *Fuel* **2018**, *212*, 523–532. [[CrossRef](#)]
15. Jiang, L.; Hu, S.; Wang, Y.; Su, S.; Sun, L.; Xu, B.; He, L.; Xiang, J. Catalytic effects of inherent alkali and alkaline earth metallic species on steam gasification of biomass. *Int. J. Hydrog. Energy* **2015**, *40*, 15460–15469. [[CrossRef](#)]
16. Kajita, M.; Kimura, T.; Norinaga, K.; Li, C.Z.; Hayashi, J.I. Catalytic and noncatalytic mechanisms in steam gasification of char from the pyrolysis of biomass. *Energy Fuels* **2009**, *24*, 108–116. [[CrossRef](#)]
17. Lahijani, P.; Zainal, Z.A.; Mohamed, A.R.; Mohammadi, M. CO₂ gasification reactivity of biomass char: Catalytic influence of alkali, alkaline earth and transition metal salts. *Bioresour. Technol.* **2013**, *144*, 288–295. [[CrossRef](#)] [[PubMed](#)]
18. Dupont, C.; Jacob, S.; Marrakchy, K.O.; Hognon, C.; Grateau, M.; Labalette, F.; Da Silva Perez, D. How inorganic elements of biomass influence char steam gasification kinetics. *Energy* **2016**, *109*, 430–435. [[CrossRef](#)]
19. Kannan, M.P.; Richards, G.N. Gasification of biomass chars in carbon dioxide: dependence of gasification rate on the indigenous metal content. *Fuel* **1990**, *69*, 747–753. [[CrossRef](#)]
20. Cuervo, N.; Dufaud, O.; Torrado, D.; Bardin-Monnier, N.; Perrin, L.; Laurent, A. Experimental study and modeling of the pyrolysis of organic dusts: application to dust explosions. *Chem. Eng. Trans.* **2013**, 931–936. [[CrossRef](#)]
21. Dufour, A.; Quartassi, B.; Bounaceur, R.; Zoulalian, A. Modelling intra-particle phenomena of biomass pyrolysis. *Chem. Eng. Res. Des.* **2011**, *89*, 2136–2146. [[CrossRef](#)]
22. Gómez-Barea, A.; Leckner, B. Modeling of biomass gasification in fluidized bed. *Prog. Energy Combust. Sci.* **2010**, *36*, 444–509. [[CrossRef](#)]
23. Palumbo, A.W.; Weimer, A.W. Heat transfer-limited flash pyrolysis of woody biomass: Overall reaction rate and time analysis using an integral model with experimental support. *J. Anal. Appl. Pyrolysis* **2015**, *113*, 474–482. [[CrossRef](#)]
24. Septien, S.; Valin, S.; Dupont, C.; Peyrot, M.; Salvador, S. Effect of particle size and temperature on woody biomass fast pyrolysis at high temperature (1000–1400 °C). *Fuel* **2012**, *97*, 202–210. [[CrossRef](#)]

25. Martinez, M.G.; Dupont, C.; Thierry, S.; Meyer, X.M.; Gourdon, C. Characteristic time analysis of biomass torrefaction phenomena—Application to thermogravimetric analysis device. *Chem. Eng. Trans.* **2016**, *50*, 61–66. [CrossRef]
26. European Standards. Solid Biofuels—Determination of Ash Content (EN 14775). Available online: https://www.google.com.tw/url?sa=t&rct=j&q=&esrc=s&source=web&cd=1&ved=2ahUKewjPrM-E1t_cAhVWfd4KHUe6BNIQFjAAegQIABAC&url=https%3A%2F%2Fwww.researchgate.net%2Fprofile%2FAIain_Celzard%2Fpost%2FWhich_ASTM_standard_should_I_refer_to_in_order_to_determine_the_moisture_and_volatiles_content_in_biomass%2Fattachment%2F59d62117c49f478072e9848e%2FAS%253A271759398375424%25401441803897376%2Fdownload%2FSolid%2Bbiofuels%2B-%2BDetermination%2Bof%2Bash%2Bcontent.pdf&usq=AOvVaw0FjluSmH5RWZsNzKmNjEL_ (accessed on 11 June 2018).
27. International Organization for Standardization. Solid Biofuels—Determination of Major Elements—Al, Ca, Fe, Mg, P, K, Si, Na and Ti (ISO 16967: 2015). Available online: <https://www.iso.org/standard/58065.html> (accessed on 11 June 2018).
28. Dupont, C.; Karakashov, B.; Dahou, T.; Martinez, M.G.; Saavedra, C.; Da Silva Perez, D.; Karakasova, L. Quality of agricultural waste from orchards and vineyards as feedstock for thermal processes with focus on torrefaction and gasification. *Biomass Bioenergy* **2018**. submitted.
29. Villermaux, J.; Antoine, B. Pyrolyse éclair de solides divisés dans un réacteur continu: 1. Un nouveau modèle de volatilisation thermique de particules solides. *Rev. Générale Therm.* **1980**, *227*, 851–860.
30. Di Blasi, C. Modeling chemical and physical processes of wood and biomass pyrolysis. *Prog. Energy Combust. Sci.* **2008**, *34*, 47–90. [CrossRef]
31. Nunn, T.R.; Howard, J.B.; Longwell, J.P.; Peters, W.A. Product compositions and kinetics in the rapid pyrolysis of sweet gum hardwood. *Ind. Eng. Chem. Process Des. Dev.* **1985**, *24*, 3. [CrossRef]
32. Samolada, M.C.; Vasalos, I.A. A kinetic approach to the flash pyrolysis of biomass in a fluidized bed reactor. *Fuel* **1991**, *70*, 883–889. [CrossRef]
33. Brewer, C.E.; Chuang, V.J.; Masiello, C.A.; Gonnermann, H.; Gao, X.; Dugan, B.; Driver, L.E.; Panzacchi, P.; Zygourakis, K.; Davies, C.A. New approaches to measuring biochar density and porosity. *Biomass Bioenergy* **2014**, *66*, 176–185. [CrossRef]
34. Johnsson, J.E.; Jensen, A. Effective diffusion coefficients in coal chars. *Proc. Combust. Inst.* **2000**, *28*, 2353–2359. [CrossRef]
35. Dalloz-Dubrujeaud, B.; Faure, R.; Tadriss, L.; Giraud, G. Perte de pression et vitesse minimum de fluidisation dans un lit de particules 2D. *Comptes Rendus l'Académie Sci.-Ser. IIB-Mech. Phys. Astron.* **2000**, *328*, 231–236. [CrossRef]
36. Dupont, C.; Chiriach, R.; Gauthier, G.; Toche, F. Heat capacity measurements of various biomass types and pyrolysis residues. *Fuel* **2014**, *115*, 644–651. [CrossRef]
37. Perry, R.H.; Green, D.W. *Perry's Chemical Engineers' Handbook*; McGraw-Hill: London, UK, 1998; ISBN 978-0-07-115982-1.
38. Whitaker, S. Forced convection heat transfer correlations for flow in pipes, past flat plates, single cylinders, single spheres, and for flow in packed beds and tube bundles. *AIChE J.* **1972**, *18*, 361–371. [CrossRef]
39. Fuller, E.N.; Schettler, P.D.; Giddings, J.C. New method for prediction of binary gas-phase diffusion coefficients. *Ind. Eng. Chem.* **1966**, *58*, 18–27. [CrossRef]
40. Kan, T.; Strezov, V.; Evans, T.J. Lignocellulosic biomass pyrolysis: A review of product properties and effects of pyrolysis parameters. *Renew. Sustain. Energy Rev.* **2016**, *57*, 1126–1140. [CrossRef]
41. Anca-Couce, A. Reaction mechanisms and multi-scale modelling of lignocellulosic biomass pyrolysis. *Prog. Energy Combust. Sci.* **2016**, *53*, 41–79. [CrossRef]
42. Deglise, X.; Donnot, A. Bois énergie—Propriétés et voies de valorisation. *Tech. Ing. Énerg. Renouvelables* **2017**. Available online: <https://www.techniques-ingenieur.fr/base-documentaire/energies-th4/energies-renouvelables-42594210/bois-energie-be8535/> (accessed on 11 June 2018).
43. Zhang, Y.; Ashizawa, M.; Kajitani, S.; Miura, K. Proposal of a semi-empirical kinetic model to reconcile with gasification reactivity profiles of biomass chars. *Fuel* **2008**, *87*, 475–481. [CrossRef]

